

Feasibility of RF Sputtering and PIIID for Production of Thin Films from Red Mud

Maria Lúcia Pereira Antunes^{a*}, Nilson Cristino da Cruz^a, Adriana de Oliveira Delgado^b, Steven Frederick Durrant^a, José Roberto Ribeiro Bortoleto^a, Vivian Faria Lima^a, Pericles Lopes Santana^a, Luciano Casel^c, Elidiane Cipriano Rangel^a

^aUniversidade Estadual Paulista – UNESP, Av. Três de Março, 511,
CEP 18087-180, Sorocaba, SP, Brasil

^bUniversidade Federal de São Carlos – UFSCar, Rod. João Leme dos Santos, km 110,
CEP 18052-780, Sorocaba, SP, Brasil

^cUniversidade Federal de São Paulo – UNIFESP, Rua Artur Riedel,
CEP 09972-970, Diadema, SP, Brasil

Received: April 15, 2014; Revised: October 3, 2014

During the extraction of aluminum from bauxite, a waste of oxides containing traces of heavy metals in a highly alkaline matrix, called Red Mud (RM), is produced. In this study RM is characterized and the feasibility of using it as a precursor for the production of thin films by Plasma Sputtering and by Plasma Immersion Ion Implantation and Deposition (PIIID) is demonstrated. The chemical structure and composition, surface morphology, topography, and wettability of the films prepared using such methodologies were investigated. The films consist mainly of the elements aluminum, silicon, iron and carbon. Infrared spectroscopic analyses reveal the presence of C=O, C-H₂, Fe(OH), Al-O and Si-C functionalities. RF Sputtering produced films with smoother surfaces, whereas PIIID produced granular surface structures. Surface contact angle measurements showed that despite the presence of oxides and hydroxides, the films are hydrophobic, thus exhibiting an interesting link between the physical and thermodynamical properties.

Keywords: *red mud, thin films, plasma sputtering, PIIID*

1. Introduction

Bauxite is the ore from which aluminum is produced. The majority of the world's bauxite reserves are located in tropical and subtropical regions¹. Brazil produces a third of the world's bauxite, being surpassed only by Australia and China. The production of aluminum begins with the extraction of alumina from bauxite ore via the Bayer process, followed by its electrolytic reduction to metallic aluminum. The Bayer process separates aluminum oxides/hydroxides from iron, titanium and silicon oxide/hydroxide species present in bauxite, using a highly caustic solution of sodium hydroxide at elevated temperatures and pressures. During this process, the waste components of the bauxite ore are separated, generating an insoluble residue called Red Mud², which is a complex slurry of mixed oxides with traces of heavy metals in a highly alkaline matrix. This hazardous residue cannot be directly disposed of in nature, thus necessitating its storage, for an open-ended time, in specially designed reservoirs to avoid the contamination of rivers and soils. Owing to the great volume of effluent generated (which increases annually) and to the continuing necessity to make preventive inspections, this requirement increases the cost of aluminum production. Indeed, the safe disposal and reuse of RM have attracted much attention in recent years³.

This internationally recognized but still unsolved problem, nevertheless, could be transformed into an advantage if a simple and cost effective methodology to reuse this residue was developed. One possibility is the use of this material to produce thin films. Its component compounds (SiO₂, Al₂O₃ and TiO₂) are already employed as film precursors⁴⁻⁶.

The first relevant literature report in this regard is due to Sutar and coworkers⁷, who used the thermal plasma spraying technique to deposit ceramic coatings from RM. In another report, Satapathy et al.⁸, showed the viability of preparing mixed oxide films on aluminum, stainless steel, mild steel and copper substrates by plasma spraying RM powder. Hybrid ceramic materials composed of TiO₂, SiO₂, FeO₂ crystalline phases and possessing high wear resistance; good adhesion strength and properties very similar to those found in ceramics were synthesized, thus demonstrating the feasibility of replacing the conventionally used compounds for ceramic production by Red Mud in plasma spray deposition. Furthermore, Prasad et al.⁹ investigated plasma sprayed RM coatings, reporting some potential applications for them as protective coatings. In all these investigations the limitation of the plasma sprayed RM coating is related to pores, cavities and cracks along the film-substrate interface. These defects are generated because of the mismatch

*e-mail: malu@sorocaba.unesp.br

between the thermal expansion coefficient of the coating and the substrate during the thermal plasma deposition, which decreases the adhesion strength⁸. Therefore a low temperature deposition technique in which energetic and reactive species of RM were generated would be especially attractive in this case.

Nielsen and co-worker¹⁰ have proposed an easy and innovative way of depositing alumina films from low temperature plasmas using a powder precursor, the Aluminum Acetylacetonate. In this case the organometallic compound is spread directly over the lower electrode of a capacitively-coupled plasma reactor while substrates are fixed on the upper one. Argon is introduced and the plasma is generated by the application of radiofrequency power to the lower electrode containing the precursor powder. The upper electrode is grounded. The self-bias polarization induced in the driven electrode promotes ion bombardment and then sputtering of the compound, providing precursors for film deposition in the plasma phase. It was demonstrated in this work that it is possible to control the amount of sputtered material and, consequently, the properties of the films by adjusting the plasma excitation parameters.

Considering such findings, the proposal of the present work is firstly to characterize the Brazilian Red Mud, and to investigate the feasibility of using it as a precursor for the production of low temperature plasma sputtered thin films employing the methodology developed by Nielsen et al.¹⁰. The approach is novel, and may find application in the production of films from what is otherwise a waste product.

2. Experimental

2.1. Characterization of Brazilian Red Mud

Red Mud was supplied by the aluminum plant located at Aluminio City, São Paulo State, Brazil. A procedure that employed inductively coupled plasma mass spectrometry (ICPMS) to determine the chemical composition of RM was reported by Antunes et al.¹¹.

The pH of RM was determined using a YSI meter calibrated with standard solutions. Infrared reflectance-absorbance spectroscopy was employed to investigate the chemical structure of RM using a JASCO FTIR-410 spectrometer. A Phillips CM200 Transmission Electron Microscope (TEM), equipped with an energy dispersive X-ray spectrometer (EDS), was used to examine the morphology of RM.

2.2. Deposition procedure

Figure 1 show the experimental apparatus employed in this work¹². The plasma reactor consists of a stainless-steel vacuum chamber fitted with two horizontal, circular stainless steel parallel-plate electrodes. In this system, the axial inter-electrode distance is of 5 cm. Prior each deposition, the reactor is evacuated continuously using a rotary vane pump (Edwards 25m³h⁻¹).

Polished stainless steel plates were used as substrates. These were chemically cleaned in a sequence of ultrasonic baths¹³, first using a detergent (DETLIMP S32) solution for 20 minutes. The plates were then rinsed individually in flowing tap water and submitted to two other ultrasonic baths for 20 minutes: first in distilled water and second in isopropyl alcohol. The substrates were finally dried in a

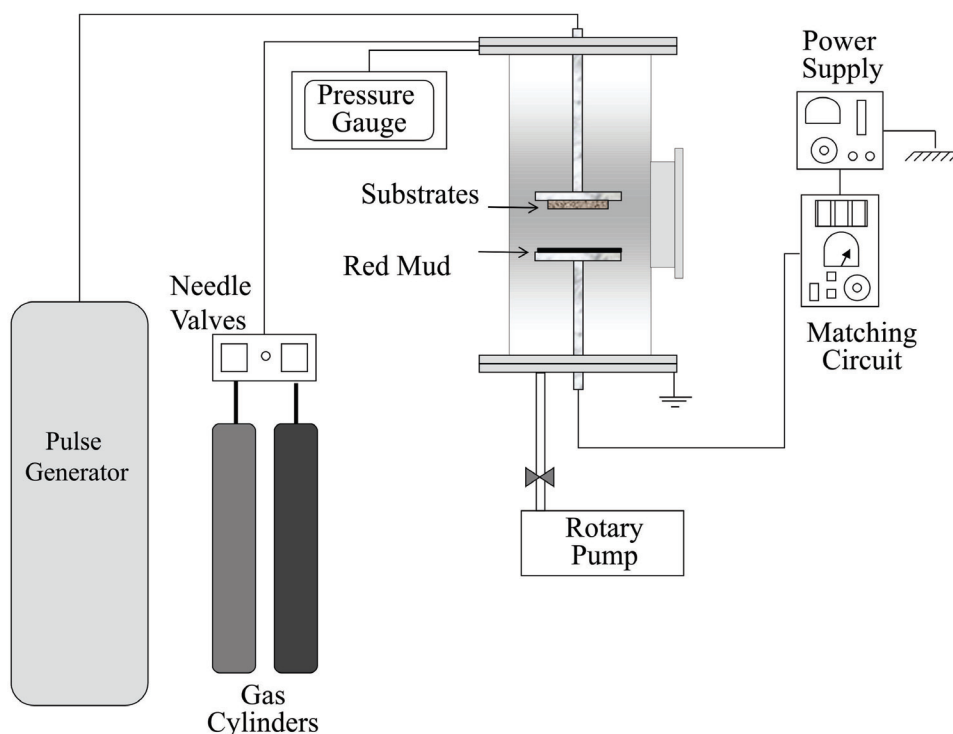


Figure 1. Schematic representation of the film deposition system.

hot air flow. The cleaned substrates were attached to the upper electrode of the plasma reactor using double-sided tape and 0.8 g of RM powder was spread directly on the lower electrode. The RM was dried at 100°C to produce a powder.

Argon was fed to the chamber from a cylinder passing through a needle valve to produce a pressure of 1.4 Pa, and the plasma was ignited by the application of radiofrequency power (13.56 MHz, 150 W) to the lowermost electrode. Two deposition methods were employed. In the first, the sputtering of the red mud components by ionic bombardment provides precursor species for film growth. This method was named *RF sputtering*.

Deposition was also accomplished in the same reactor configuration but using in addition a pulsed bias voltage applied to the upper electrode. Square-wave high voltage negative pulses (1.5 kV, 300 Hz) were supplied to the sample holder (upper electrode) to promote ion bombardment of the growing layer (PIIID). In both cases deposition time was 5400 s.

2.3. Film characterization

Surface wettability was determined from contact angle (θ) data taken using a Ramé-Hart 100 goniometer. These measurements were conducted after ageing the samples in atmospheric conditions for two months. Three drops of deionized water (0.2 μ L) were deposited on different regions of the sample surface and the contact angle was measured 10 times on each side of the drop, resulting in sixty θ values per sample.

Film thickness was measured using a profile meter on samples deposited onto smooth glass plates containing a film step-height delineated during the deposition process with the aid of a mask. Thickness was also estimated using the transversal view of the samples in micrographs acquired in a Jeol JSM-6010LA scanning electron microscope equipped with a secondary electrons detector.

Polarization-modulation Infrared Reflection Absorption Spectroscopy (PM-IRRAS) was used to characterize the chemical structure of the films. PM-IRRAS is a powerful technique for analyzing thin films supported on solid substrates¹⁴⁻¹⁶. The PM-IRRAS measurements were taken using a KSV PMI 550 Instrument.

Surface topography was evaluated using atomic force microscopy, AFM, in air using a XE-100 instrument from Park Systems. Images (5 mm \times 5 mm and 2 mm \times 2 mm) of each sample were acquired in non-contact mode using 512 \times 512 pixels. For this, silicon tips of 5 nm nominal radius were assembled on cantilevers with a resonance frequency \geq 200 kHz. From the images the root mean square roughness, W_{RMS} , was determined as defined by Equation 1.

$$w_{RMS} = \sqrt{\frac{1}{N} \sum_{i=1}^N (h_i - \bar{h})^2} \quad (1)$$

where N is the total number of pixels, h_i is the height of each pixel in the image and \bar{h} is the average height over the scanned area.

3. Results and Discussion

3.1. Characterization of Brazilian Red Mud

The composition of RM, as determined using ICPMS, is presented in Table 1. Iron, aluminum and silicon oxides are the main components, making up half of the chemical composition. All of these major compounds are relevant precursors of film formation.

The high alkalinity of RM is confirmed by the pH measurements, 10.0 ± 0.5 , and is attributed to the presence of NaOH in the Bayer Process.

An infrared spectrum of RM is depicted in Figure 2. Absorptions related to different carbonates groups and species which have a dawsonite-like structure are observed between 1600 and 1400 cm^{-1} [17]. The presence of silicon, iron and aluminum oxides is revealed by the wide band lying between 890 and 1100 cm^{-1} [18-20]. These results are consistent with the composition of RM presented in Table 1.

Figure 3 shows the morphology of RM particles observed in TEM images. It is possible to observe particles with different sizes and forms. The smaller particles (50 nm of diameter) were identified by EDS as iron particles, while the larger particles were identified as consisting of silicon compounds.

3.2. Film characterization

A clear difference in color was visible to the naked eye, between the clean substrates and the plasma-exposed substrates. The color changed from that of the usual aspect of stainless steel to a light brown. Thickness of the films deposited by RF sputtering was, accordingly to profilometry data, equal to (34 ± 10) nm while that prepared by PIIID was substantially thicker, (520 ± 150) nm. Figure 4 shows a representative transversal view of the sample prepared by PIIID. Owing to the lower thickness of the RF sputtered film, it was not possible to visualize it in the transversal micrograph of the substrate surface. The deposition rate can be obtained from the ratio between thickness and deposition time, t , which was 5400 s. For the PIIID samples, the deposition rate was 5.8 nm/min, and that of the RF sputtered was 0.4 nm/min. These values are substantially lower than the obtained by plasma spray depositions (300-500 nm/min)⁸

Table 1. Chemical Composition of Brazilian Red Mud.

Oxide	(m/m %)
SiO ₂	19.2
Al ₂ O ₃	22.8
Fe ₂ O ₃	27.4
TiO ₂	3.0
MnO	0.2
MgO	0.4
CaO	2.2
Na ₂ O	7.9
K ₂ O	0.8
P ₂ O ₅	0.4
LOI*	15.5
Total	99.8

*Loss on ignition.

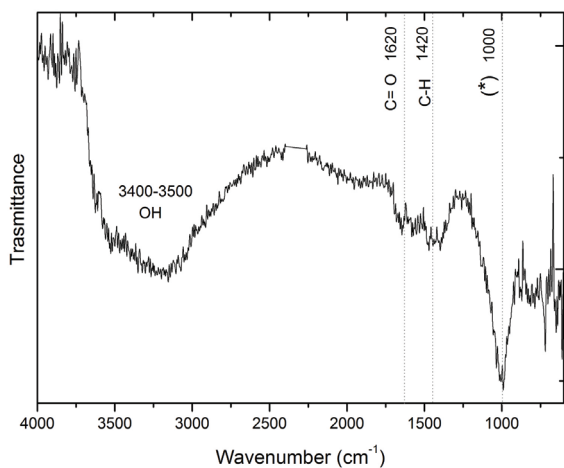


Figure 2. FTIR spectrum of red mud. (*) Band attributed to ν Si-O, δ FeOOH and Al_2O_3 .

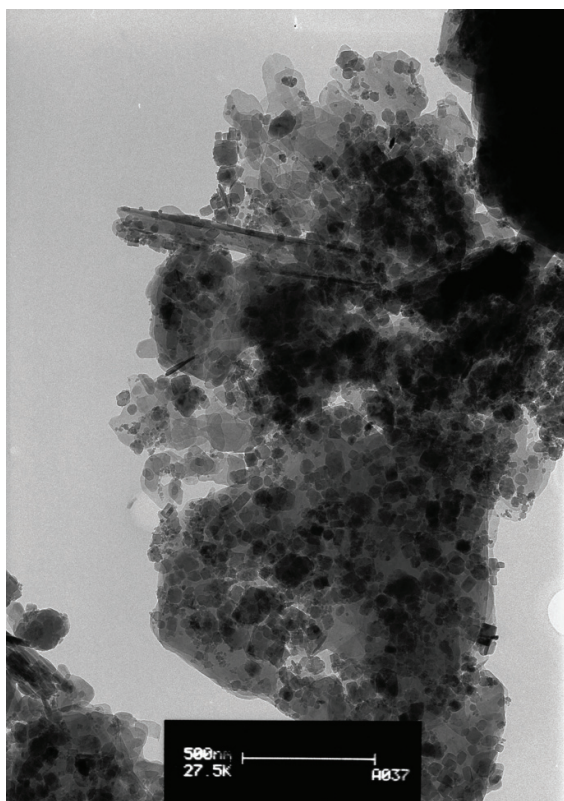


Figure 3. TEM of red mud.

but considerably lower power densities are also involved in the low temperature plasma deposition procedures.

To understand the discrepancies between the results obtained by RF sputtering and PIID, recall that film formation depends on the availability of film precursors in the plasma, which in turn depends on the sputtering yield. Once material from RM is mobilized to the plasma, further activation may produce excited species, free radicals, and ions. Deposition occurs when these or similar species arrive at the surface of the substrate.

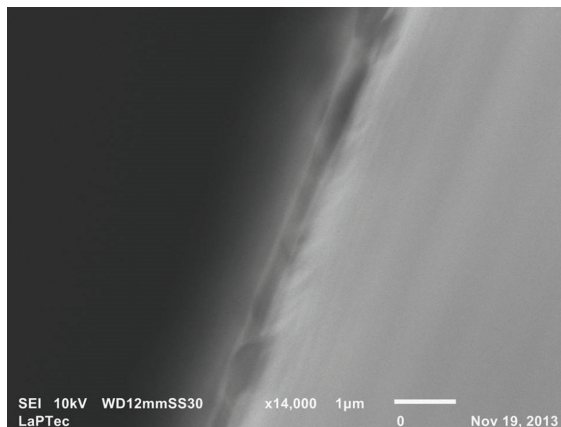


Figure 4. SEM of films obtained by PIID.

As the applied power employed was maintained constant for the two methods (RF sputtering and PIID), the amount of sputtering is postulated to be roughly the same. Despite this similarity, the rate at which positively charged ions arrive at the substrate is greatly increased in PIID, in which negative pulses are applied to the samples, thereby directing positive ions towards them. Consequently, in PIID greater numbers of film-forming species impinge on the substrate and on the growing film, thus increasing the deposition rate.

The surface contact angle of the films is depicted in Figure 5. The contact angle for the bare stainless steel substrate, also presented in the figure, increases from 62° to 88° as the steel surface is submitted to RF sputtering. Still greater, hydrophobic, contact angles ($> 100^\circ$) are obtained from the surfaces exposed to PIID.

Two parameters should be considered to interpret these results: chemical composition and surface topography. To evaluate the chemical composition and molecular structure of the films, their polarization-modulation infrared spectra are presented in Figure 6 in the 2700 to 3200 cm^{-1} range.

Contributions related to C-H stretching vibrations in CH_2 species are detected at 2920 and 2850 cm^{-1} [21]. These groups can originate from the organic content of RM as demonstrated by both the infrared spectra (Figure 2) and ICPMS data (Table 1). According to the latter the red mud contains a relatively high amount of organic materials (15.5% m/m).

Figure 7 shows the PM-infrared spectra of the films in the 800 to 1200 cm^{-1} interval. The wide band lying at 1000 cm^{-1} is tentatively attributed to the Si-O asymmetric stretching vibration in Si-O-Si groups (1030 cm^{-1}),^{18,19} to the O-H deformation vibration in FeOOH (1010 cm^{-1})²⁰, and to the stretching of Al=O (1027 cm^{-1})²².

The other, a large and intense band lying below 1000 cm^{-1} , was also observed in the work of Yamada-Takamura et al.²³ and Nguyen et al.²⁴ and is characteristic of amorphous alumina.

As deposition is performed under ion bombardment, the band in the low wavenumber region can be resolved into peaks centered at 820 , 850 and 870 cm^{-1} . The first derives from the stretching vibration of Si-C²⁵, the second originates from the stretching vibration of Al-O in alumina²⁶, while

the last is ascribed to an O-H vibration in FeOH¹⁷. The confirmation of the presence of silicon, together with the presence of C-H groups, detected in the IR bands of Figure 2, suggests that silicon may be bonded to carbon.

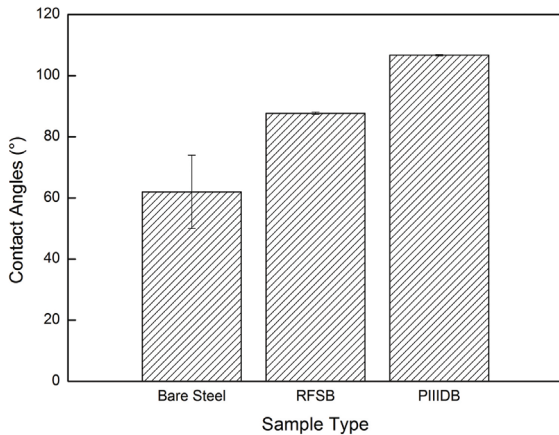


Figure 5. Contact angle for films deposited from red mud.

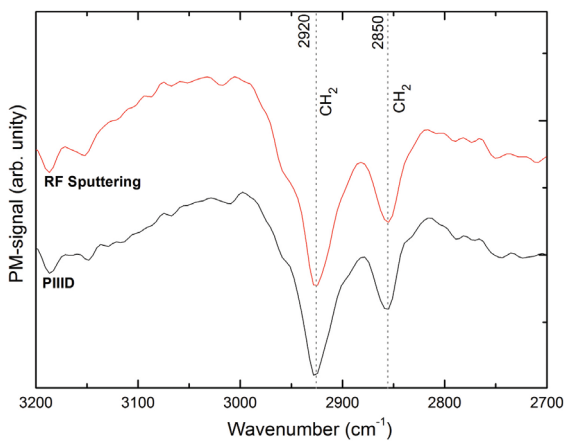


Figure 6. PM-IRRAS spectra for RF Sputtered and PIIBD film (2700-3200cm⁻¹).

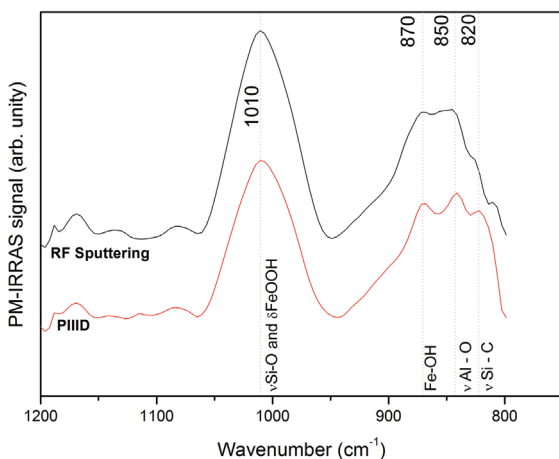


Figure 7. PM-IRRAS spectra for RF Sputtered and PIIBD film (800-1200cm⁻¹).

The molecular structure and chemical composition of the films is consistent with the composition of RM. Interestingly, the most abundant elements in RM, that is Fe₂O₃ (27.4%), Al₂O₃ (22.8%), SiO₂ (19.2%) and organic material (15.5%), are also detected in the film structure. Manganese and Magnesium were not detected in the structure as a consequence of their low proportions in RM and low sputtering rates. In summary, the film is a hybrid material composed of different oxides/hydroxides, with organic inclusions, as observed in the work of Satapathy et al.⁸. Coatings similar to these were also obtained by electrolytic plasma oxidation of carbon steel substrates in an aluminate-sodium hydroxide (NaAlO₂+ NaOH) electrolyte¹⁷, the Fe₂O₃ species provided, in this case, by the substrate. Thus, when the molecular structure of the coatings obtained in both studies is compared, RM also appears as a promising compound to replace the aluminate and sodium hydroxide used in the electrolytic plasma oxidation approach.

Considering that the films prepared in the present work are composed by oxides and hydroxides, it would be expected that surface was hydrophilic. However, evidence was found that apolar methyl groups are present, probably connected to the silicon oxide functionality since Si-C groups are detected by infrared spectroscopy. Furthermore, they may establish connections with aluminum network too, as observed in the work of Benjamin et al.⁵. The apolar methyl groups promote a shielding effect on the polar molecules as they surround it^{10,27} providing low receptivity towards water and polar liquids in general.

Another aspect relevant to the water wettability is the surface topography and morphology. Figure 8 shows atomic force microscopy images of films prepared in this work as well as of the bare substrate. The stainless steel presents defects (Figure 8a) characteristic of the material structure and finishing. As RF sputtering proceeds, the surface became smoothed (Figure 8b) but still present some defects, which may be ascribed to substrate irregularities not hidden by the thin deposited layer. However, as the holes have greater diameters than those found in the bare steel and are distributed over all of the sample surface it seems more probable that they originate from the films, very similar to those found in ceramic materials²⁸. When the deposition is conducted under ion bombardment (Figure 8c) a drastic evolution from a more uniform surface to a granular one is observed. Owing to the reduced film thickness the imperfections of the substrate are still detected.

In addition to its effect on the deposition rate, ion bombardment also affects the morphology of the material. The impingement of fast ions on the substrate surface increases the concentration of surface defects that act as nucleation centers of film growth. This has already been reported in the literature for vapor phase deposition²⁹ and is here suggested to be responsible for the observed morphological changes.

The root mean square roughness of the films, W_{RMS} , generated from AFM images, is presented in Figure 9. Consistently with the morphological evolution observed in the structure, the W_{RMS} increases when the deposition is performed under ion bombardment.

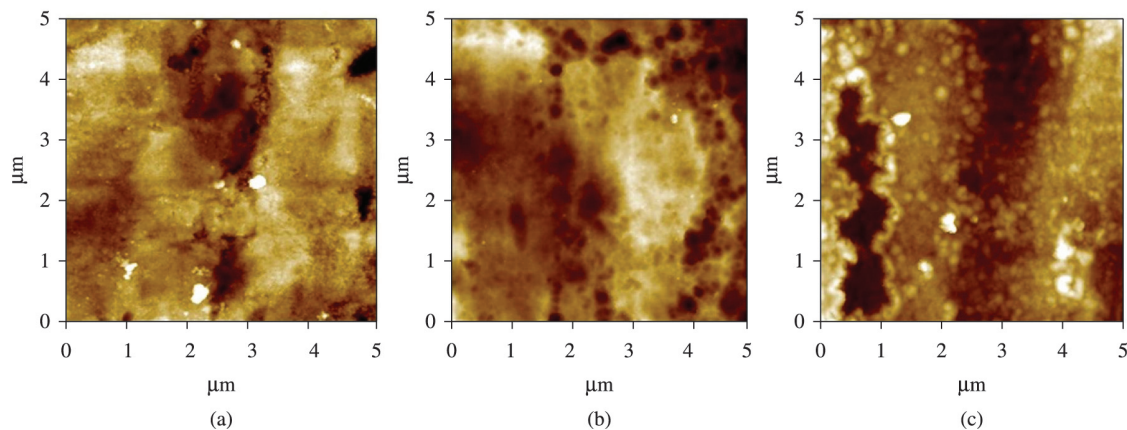


Figure 8. Atomic force microscopy images of (a) the bare substrate, (b) RF sputtered film and (c) PIID film.

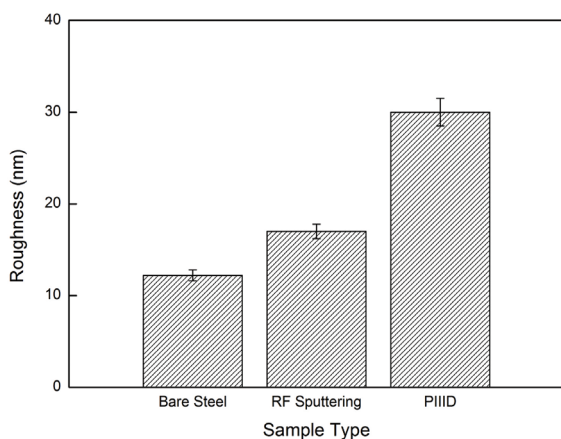


Figure 9. Root mean square surface roughness for the different sample types.

Therefore, in addition to changes in the chemical composition, the evolution of the surface roughness can also contribute to the enhancement in the hydrophobic character of the samples. It is recognized that an elevation in the surface roughness of naturally hydrophobic surfaces tends to further increase their contact angle³⁰.

4. Conclusions

The results presented here demonstrated that it is possible to prepare films from RM powder using low temperature plasmas. In addition to being innovative and feasible in any plasma system this methodology enables the reuse of an important residue. Under the conditions employed here, an argon plasma was able to sputter RM species into the plasma phase, enabling the deposition of thin layers constituted by a complex of organics, oxides and hydroxides.

Although deposition rate was low, the material obtained from these methodologies can find application in high aggregated value devices where thin films or even few monolayers produce the desired effect as in biomaterials, microelectronic, sensors and optical devices. The possibility of controlling the surface wettability altogether with the pore diameters may make such films interesting to chemical and physical control the permeability of species in polymeric filtration membranes or to protect metals against corrosion. Owing to the low temperature involved in the processes, oxide-containing films can be deposited onto the surface of high temperature sensitive materials, such as polymers, acting as protective coatings for them.

Furthermore, by adjusting the system geometry (inter electrode distance) and the plasma excitation parameters, greater deposition rates can be attained. It is a special interest of the authors to evaluate the effect of hydrogen incorporation on the deposition kinetics. Hydrogen should reduce the stable oxides of RM thus increasing their ejection into the plasma phase. Aside from the plasma composition, gas pressure and excitation power certainly affect the sputtering yield and then the deposition kinetics. New studies will be performed to systematically address these questions, aiming to optimize the sputtering rate as well as its selectivity, so as to control the composition of the films.

Despite its slight effect on molecular structure, low energy ion bombardment affected the deposition kinetics, resulting in thicker, rougher and hydrophobic films. Further efforts will be devoted to investigate the effect of higher energy and fluence ion bombardment on the film properties, especially on the carbon content, crystalline phase precipitation, mechanical and tribological properties.

Acknowledgements

FAPESP – Proc. N° 2012/14708-2; Proc. N° 2013/06210-7; CNPq – Proc. N° 301622/2012-4.

References

1. Smith P. The processing of high silica bauxites – Review of existing and potential process. *Hydrometallurgy*. 2009; 98(1-2):162-176. <http://dx.doi.org/10.1016/j.hydromet.2009.04.015>.
2. Hind AR, Bhargava SK and Grocott SC. The surface chemistry of Bayer process solids: a review. *Colloids and Surfaces. A, Physicochemical and Engineering Aspects*. 1999; 146(1-3):359-374. [http://dx.doi.org/10.1016/S0927-7757\(98\)00798-5](http://dx.doi.org/10.1016/S0927-7757(98)00798-5).
3. Wang S, Ang HM and Tadó MO. Novel applications of red mud as coagulant, adsorbent and catalyst for environmentally benign processes. *Chemosphere*. 2008; 72(11):1621-1635. <http://dx.doi.org/10.1016/j.chemosphere.2008.05.013>. PMID:18558418
4. Vassallo E, Cremona A, Laguardia L and Mesto E. Preparation of plasma-polymerized SiO_x-like thin films from a mixture of hexamethyldisiloxane and oxygen to improve the corrosion behavior. *Surface and Coatings Technology*. 2006; 200(9):3035-3040. <http://dx.doi.org/10.1016/j.surfcoat.2004.11.001>.
5. Schmidt BW, Rogers BR, Gren CK and Hanusa TP. Carbon incorporation in chemical vapor deposited aluminum oxide films. *Thin Solid Films*. 2010; 518(14):3658-3663. <http://dx.doi.org/10.1016/j.tsf.2009.09.105>.
6. Zhang M, Lin G, Dong C and Wen L. Amorphous TiO₂ films with high refractive index deposited by pulsed bias arc ion plating. *Surface and Coatings Technology*. 2007; 201(16-17):7252-7258. <http://dx.doi.org/10.1016/j.surfcoat.2007.01.043>.
7. Sutar H, Mishra SC, Sahoo SK, Satapathy A and Kumar V. Morphology and solid particle erosion wear behavior of red mud composite coatings. *Natural Science*. 2012; 4(11):832-838. <http://dx.doi.org/10.4236/ns.2012.411111>.
8. Satapathy A, Sutar H, Mishra SC and Sahoo SK. Characterization of Plasma sprayed pure red mud coatings: An analysis. *American Chemical Science Journal*. 2013; 3(2):151-163. <http://dx.doi.org/10.9734/ACSJ/2013/3218>.
9. Prasad N, Sutar H, Mishra HC, Sahoo SK and Acharya SK. Dry sliding wear behavior aluminium matrix composite using red mud an industrial waste. *International Research Journal of pure and applied chemistry*. 2013; 3(1):59-74. <http://dx.doi.org/10.9734/IRJPAC/2013/2906>.
10. Nielsen GF, Silva LHF, Cruz NC and Rangel EC. Preparation of films from aluminum acetylacetonate by plasma sputtering. *Surface and Interface Analysis*. 2013; 45(7):1113-1118. <http://dx.doi.org/10.1002/sia.5236>.
11. Antunes MLP, Couperthwaite SJ, Conceição FT, Jesus CPC, Kiyohara PK, Coelho ACV, et al. Red Mud from Brazil: Thermal behavior and Physical Properties. *Industrial & Engineering Chemistry Research*. 2012; 51(2):775-779. <http://dx.doi.org/10.1021/ie201700k>.
12. Rangel RCC, Souza MEP, Schreiner WH, Freire CMA, Rangel EC and Cruz NC. Effect of the fluorination of DLC film on the corrosion protection of aluminum alloy AA5052. *Surface and Coatings Technology*. 2010; 204(18-19):3022-3028. <http://dx.doi.org/10.1016/j.surfcoat.2010.03.055>.
13. Mancini SD, Nogueira AR, Rangel EC and Cruz NC. Solid-state hydrolysis of postconsumer polyethylene after plasma treatment. *Journal of Applied Polymer Science*. 2013; 127(3):1989-1996. <http://dx.doi.org/10.1002/app.37591>.
14. Caseli L, Gruber J, Li RWC and Péres LO. Investigation of the conformational changes of a conducting polymer in gas sensor active layers by means of polarization-modulation infrared reflection absorption spectroscopy (PM-IRRAS). *Langmuir*. 2013; 29(8):2640-2645. <http://dx.doi.org/10.1021/la3050797>. PMID:23373530
15. Brosseau CL, Leitch J, Bin X, Chen M, Roscoe SG and Lipkowski J. Electrochemical and PM-IRRAS a glycolipid-containing biomimetic membrane prepared using Langmuir-Blodgett/Langmuir-Schaefer deposition. *Langmuir*. 2008; 24(22):13058-13067. <http://dx.doi.org/10.1021/la802201h>. PMID:18925767
16. Ramin MA, Le Bourdon G, Daugey N, Bennetau B, Vellutini L and Buffeteau T. PM-IRRAS investigation of self-assembled monolayers grafted onto SiO₂/Au substrates. *Langmuir*. 2011; 27(10):6076-6084. <http://dx.doi.org/10.1021/la2006293>. PMID:21486004
17. Karpushenkov SA, Shchukin GL, Belanovich AL, Savenko VP and Kulak AI. Plasma electrolytic ceramic-like aluminum oxide coatings on iron. *Journal of Applied Electrochemistry*. 2010; 40(2):365-374. <http://dx.doi.org/10.1007/s10800-009-0005-1>.
18. Gengenbach TR and Griesser HJ. Post-deposition ageing reactions differ markedly between plasma polymers deposited from siloxane and silazane monomers. *Polymer*. 1999; 40(18):5079-5094. [http://dx.doi.org/10.1016/S0032-3861\(98\)00727-7](http://dx.doi.org/10.1016/S0032-3861(98)00727-7).
19. Francassi F, D'Agostino R, Palumbo F, Angelini E, Grassini S and Rosalbino F. Application of plasma deposited organosilicon thin films for the corrosion protection of metals. *Surface and Coatings Technology*. 2003; 174-175:107-111. [http://dx.doi.org/10.1016/S0257-8972\(03\)00422-5](http://dx.doi.org/10.1016/S0257-8972(03)00422-5).
20. Jasinski R and Lob A. FTIR Measurements of iron oxides on low alloy steel. *Journal of the Electrochemical Society*. 1988; 135(3):551-556. <http://dx.doi.org/10.1149/1.2095656>.
21. Caseli L, Sousa-Martins D, Maia M, Lima-Filho AAS, Rodrigues EB and Belfort R Jr. An intraocular dye solution based on lutein and zeaxanthin in a surrogate internal limiting membrane model: a Langmuir monolayer study. *Colloids and Surfaces B: Biointerfaces*. 2013; 107:124-129. <http://dx.doi.org/10.1016/j.colsurfb.2013.01.076>. PMID:23475059
22. Ram S. Infrared spectral study of molecular vibrations in amorphous, nanocrystalline and AlO(OH)·nH₂O bulk crystals. *Infrared Physics & Technology*. 2001; 42(6):547-560. [http://dx.doi.org/10.1016/S1350-4495\(01\)00117-7](http://dx.doi.org/10.1016/S1350-4495(01)00117-7).
23. Yamada-Takamura Y, Koch F, Maier H and Bolt H. Characterization of alpha-phase aluminum oxide films deposited by filtered vacuum arc. *Surface and Coatings Technology*. 2001; 142-144:260-264. [http://dx.doi.org/10.1016/S0257-8972\(01\)01206-3](http://dx.doi.org/10.1016/S0257-8972(01)01206-3).
24. Nguyen QT, Kidder JN Jr and Ehrman SH. Hybrid gas-to-particle conversion and chemical vapor deposition for the production of porous alumina films. *Thin Solid Films*. 2002; 410(1-2):42-52. [http://dx.doi.org/10.1016/S0040-6090\(02\)00239-0](http://dx.doi.org/10.1016/S0040-6090(02)00239-0).
25. Rao AP and Rao AV. Modifying the surface energy and hydrophobicity of the low density silica aerogels through the use of combinations of surface-modification agents. *Journal of Materials Science*. 2010; 41(1):51-63.
26. Chrissou CE and Pitt CW. Al₂O₃ thin films by plasma-enhanced chemical vapor deposition using trimethyl-amine alane (TMAA) as the Al precursor. *Applied Physics A: Materials Science & Processing*. 1997; 65(4-5):469-475. <http://dx.doi.org/10.1007/s003390050611>.
27. Lopes BB, Rangel RCC, Antonio CA, Durrant SF, Cruz NC and Rangel EC. Nanoindentation. In: *Proceedings of International Conference on Innovative Technologies*; 2012; Rijeka, Croatia. Rijeka: Nemecek; 2012. p. 179-187.
28. Natali M, Carta G, Rigato V, Rossetto G, Salmaso G and Zanella P. Chemical, morphological and nano-mechanical characterization of Al₂O₃ thin films deposited by metal

- organic chemical vapor deposition on AISI304 stainless steel. *Electrochimica Acta*. 2005; 50(23):4615-4620. <http://dx.doi.org/10.1016/j.electacta.2004.10.097>.
29. Esch S, Bott M, Michely T and Comsa G. Nucleation homoepitaxial films grown with ion assistance on Pt(111). *Applied Physics Letters*. 1995; 67:3209-3211. <http://dx.doi.org/10.1063/1.115165>.
30. Wenzel RN. Resistance of solid surfaces to wetting by water. *Industrial & Engineering Chemistry*. 1936; 28(8):988-994. <http://dx.doi.org/10.1021/ie50320a024>.